

Synthesis of Nanoparticles Using *Euphorbia prostrata* Extract Reveals a Shift from Apoptosis to G0/G1 Arrest in *Leishmania donovani*

Abdul Abdus Zahir^{1#}, Indira Singh Chauhan^{2#}, Asokan Bagavan¹, Chinnaperumal Kamaraj¹, Gandhi Elango¹, Jai Shankar⁴, Nidhi Arjaria⁴, Mohana Roopan³, Abdul Abdul Rahuman^{1*} and Neeloo Singh^{2*}

¹Unit of Nanotechnology and Bioactive Natural Products, Post Graduate and Research Department of Zoology, C. Abdul Hakeem College, Melvisharam-632509, Vellore District, Tamil Nadu, India

²Biochemistry Division, CSIR Central Drug Research Institute, Jankipuram Extension, Sitapur Road, Lucknow- 226031, India

³Organic & Medicinal Chemistry Research Laboratory, Organic Chemistry Division, School of Advanced Sciences, VIT University, Vellore-632 014, Tamil Nadu, India

⁴Transmission Electron Microscopy, CSIR Indian Institute of Toxicology Research, M.G. Marg Lucknow-226001, India

*Contributed equally as joint first authors

Abstract

The aim of the present investigation was to synthesize silver (Ag) and titanium dioxide (TiO₂) nanoparticles (NPs) using the aqueous leaves extract of *Euphorbia prostrata* as antileishmanial agents and to explore the mechanism of induced cell death. *In vitro* antileishmanial activity of synthesized NPs was tested against promastigotes of *Leishmania donovani* by alamar Blue[®] cell viability reagent and propidium iodide uptake assay. The effective leishmanicidal activity of synthesized Ag NPs was further confirmed by cell cycle progression, externalized phosphatidylserine, DNA fragmentation assay, reactive oxygen species (ROS) level, intracellular non-protein thiols and transmission electron microscopy (TEM) of the treated parasites. TEM analysis of the synthesized Ag NPs and TiO₂ NPs showed spherical shape with an average size of 12.82 ± 2.50 and 83.22 ± 1.50 nm, respectively. Ag NPs was found to be the most active agent against *Leishmania* parasites after 24 h exposure with IC₅₀ value of 14.94 µg/mL. A significant increase in G0/G1 phase of the cell cycle with subsequent decrease in S and G2/M phases was observed when compared to control and thus confirming the growth inhibitory effect of synthesized Ag NPs. Decreased ROS level was also observed which could be responsible for caspase independent shift from apoptosis (G0/G1 arrest) to massive necrosis. High molecular weight DNA fragmentation as a positive consequence of necrotic cell death was also visualized. In the present study, the unique trypanothione/trypanothione reductase (TR) system of *Leishmania* cells was significantly inhibited by synthesized Ag NPs was reported. The green synthesized Ag NPs may provide promising leads for the development of cost effective and safer alternative treatment against visceral leishmaniasis.

Keywords: *Euphorbia prostrata*; Synthesized nanoparticles; *Leishmania donovani*; Cell cycle arrest; Trypanothione reductase; Transmission electron microscopy; Chemotherapy

Introduction

Neglected diseases caused by parasites are the second cause of mortality and impose a substantial burden of morbidity round the globe and more predominantly in the developing countries. Leishmaniasis currently threatens 350 million people in 88 countries around the world. Two million new cases are considered to occur annually, with an estimated 12 million people presently infected [1]. Among different leishmanial infections, Visceral leishmaniasis (VL) caused by *Leishmania donovani* is the most threatening parasite. Although miltefosine and amphotericin B are used for clinical treatment, the antileishmanial drug arsenal still requires improvement [2]. For instance, miltefosine monotherapy has failed to cure relapsing VL in HIV-infected patients and thus its role against the HIV-associated VL remains unclear [3].

Nanomedicine is defining the use of nanotechnology in medicine, which has been of great interest in recent years. The use of nanoparticles (NPs) for therapeutics is one of the purposes of nanomedicine [4,5]. In recent years, an increasing percentage of nanomaterials are emerging and making advancement in different fields. NPs play an indispensable role in drug delivery, diagnostics, imaging, sensing, gene delivery, artificial implants and tissue engineering [6]. Sinha et al. [7] have reported that the biosynthesis of NPs is advantageous over chemical and physical methods as it is a cost-effective and environment friendly method, where it is not necessary to use high pressure, energy, temperature and toxic chemicals. Silver nanoparticles (Ag NPs) have several important applications in the field of biolabelling, sensors, antimicrobial agents and filters. They are capable of purifying drinking water, degrading

pesticides and killing human pathogenic bacteria [8]. Ag NPs have been used in treatment and improvement of drug delivery against leishmaniasis [9-12]. Silver polypyridyl complexes are biologically active against *Leishmania mexicana*, where they interact with DNA [13]. Similarly, nano-preparations with titanium dioxide nanoparticles (TiO₂ NPs) are currently under investigation as novel treatments for acne vulgaris, recurrent condyloma acuminata, atopic dermatitis, hyperpigmented skin lesions and other non dermatologic diseases [14]. Recent authors investigated that the Quercetin (polyphenolic compound) conjugated gold NPs were evaluated against promastigotes and amastigotes of *L. donovani* [15].

There are limited studies concerning the green synthesis of NPs and its control efficacy against *Leishmania* parasite. Among the various

***Corresponding authors:** Abdul Abdul Rahuman, Unit of Nanotechnology and Bioactive Natural Products, Post Graduate and Research Department of Zoology, C. Abdul Hakeem College, Melvisharam-632509, Vellore District, Tamil Nadu, India, Tel: +91-9442310155; Fax: +91-041-72269487; E-mail: abdulrahuman6@hotmail.com

Neeloo Singh, Unit of Nanotechnology and Bioactive Natural Products, Post Graduate and Research Department of Zoology, C. Abdul Hakeem College, Melvisharam-632509, Vellore District, Tamil Nadu, India, Tel: +91-9415002065; Fax: +91-522-22623405; E-mail: neeloo888@yahoo.com

Received June 12, 2014; Accepted July 25, 2014; Published July 30, 2014

Citation: Zahir AA, Chauhan IS, Bagavan A, Kamaraj C, Elango G, et al. (2014) Synthesis of Nanoparticles Using *Euphorbia prostrata* Extract Reveals a Shift from Apoptosis to G0/G1 Arrest in *Leishmania donovani*. J Nanomed Nanotechnol 5: 213. doi: [10.4172/2157-7439.1000213](https://doi.org/10.4172/2157-7439.1000213)

Copyright: © 2014 Zahir AA, et al. This is an open-access article distributed under the terms of the Creative Commons Attribution License, which permits unrestricted use, distribution, and reproduction in any medium, provided the original author and source are credited.

biosynthetic approaches, the use of plant extracts is preferable as they are easily available, safe to handle and possess a broad viability of metabolites. The potential of plants as biological materials for the synthesis of NPs is yet to be fully explored [16]. *Euphorbia prostrata* is a small, prostrate and hispidly pubescent annual herb found all over India. The leaves extract of *E. prostrata* showed antibacterial, nematicidal and antiparasitic activities [17]. Anthraquinones, flavonoids, phenols, phlobotannins, polysaccharides, saponins, tannins and terpenoids were isolated from the leaves extract of *E. prostrata* [18]. The flavonoids were promising compounds for controlling human and animal parasitic diseases [19]. Phenolic compounds were tested against *Leishmania* spp. and for immunomodulatory effects on macrophage [20]. Similarly, the antileishmanial activities of terpenoid derivatives were tested against promastigotes and intracellular amastigotes form of *L. donovani* [21]. In the present study, the antileishmanial activity of green synthesized Ag NPs and TiO₂ NPs using the aqueous leaves extract of *E. prostrata* were evaluated against promastigotes of *L. donovani*.

Materials and Methods

AgNO₃ and TiO(OH)₂ analytical grade were purchased from Qualigens Fine Chemicals, Mumbai, India (99.9% pure) and Himedia Laboratories Pvt. Ltd., Mumbai, India, respectively. AlamarBlue[®] cell viability reagent, 2',7'-dichloro-4,6-diamidino-2-methyl-5-carboxyfluorescein diacetate (DCFH-DA) and 5-chloromethylfluorescein-diacetate (cellTracker[™] Green CMFDA) were purchased from Invitrogen, Carlsbad, CA. Sodium cacodylate and araldite-DDSA mixture were acquired from Ladd Research Industries, USA. Propidium iodide (PI) and RNase A were purchased from Sigma-Aldrich (St. Louis, MO, USA) and Fermentas (Waltham, MA, USA), respectively. All other chemicals and reagents were obtained from Sigma-Aldrich with high purity analytical grade.

Synthesis of Ag NPs and TiO₂ NPs

Fresh leaves of *E. prostrata* were collected in and around Melvisharam, Vellore district, Tamil Nadu, India. The aqueous leaves extract was prepared by taking 2 g of finely cut leaves in 250 mL of Erlenmeyer flask along with 100 mL of sterilized double distilled water and boiling the mixture at 60°C for 15 – 20 min. The extract was filtered with Whatman filter paper no. 1, stored at –20°C and used within a week. The biosynthesis of Ag NPs was carried out using different compositions of the aqueous leaves extract with AgNO₃ solution (3:97, 6:94, 9:91, 12:88 and 15:85 mL). The reaction mixture was periodically observed for the change in color and analyzed by UV-Vis spectrophotometer in the range of 100 - 700 nm. Total volume of 88 mL of 1 mM AgNO₃ solution was reduced using 12 mL of aqueous leaves extract of *E. prostrata* at room temperature for 6 h, resulting in a brown yellow colored solution indicating the formation of Ag NPs synthesis [22]. For synthesis of TiO₂ NPs, the Erlenmeyer flask containing 100 mL of 5 mM TiO(OH)₂ was stirred for 2 h. Different concentrations of aqueous leaves extract of *E. prostrata* were prepared and interacted with the TiO(OH)₂ solution mixing ratio of 5:95, 10:90, 15:85, 20:80 and 25:75 mL, separately. 20 mL of aqueous leaves extract of *E. prostrata* was added to 80 mL of TiO(OH)₂ solution for the optimization of TiO₂ NPs synthesis. The pure TiO(OH)₂ solution and the aqueous leaves extract didn't show any color change. Whereas in the leaves extract with TiO(OH)₂ showed the change of color to light green. Different reaction parameters (concentrations of plant extract, substrate concentrations, pH, temperature and reaction time) were optimized to synthesize NPs with controlled properties [23].

Characterization of synthesized Ag NPs and TiO₂ NPs

Synthesis of NPs solution with leaves extract was observed by

UV-Vis spectroscopy. The bioreduction of ions in the solutions was monitored by periodic sampling of aliquots (1 mL) of the aqueous component after 20 times dilution and measured in the UV-Vis spectra. Samples were monitored as a function of time of reaction using Shimadzu 1601 spectrophotometer in the 100–700 nm range operated at a resolution of 1 nm. The reduced solution centrifuged at 8000 rpm for 40 min and resulting supernatant was discarded and pellet obtained was redispersed in deionized water. Centrifugation was repeated three to five times to wash off any adsorbed substances on the surface of the synthesized NPs.

Thus obtained purified and dried pellet of synthesized Ag NPs and TiO₂ NPs were subjected to X-ray diffraction (XRD) analysis. For XRD studies, dried NPs were coated on XRD grid, and the spectra were recorded by using Phillips PW 1830 instrument operating at a voltage of 40 kV and a current of 30 mA with Cu Kα1 radiation. Fourier transform infrared (FTIR) analysis of the samples were carried out using Perkin Elmer spectrophotometer in the diffuse reflectance mode at a resolution of 4 cm⁻¹ in KBr pellets and showed possible functional groups for the formation of NPs. Topography of synthesized NPs was studied using AFM analysis (Atomic force microscopy – Veeco Innova, USA). Images have been processed using XEI software given by Park system. The synthesized NPs were examined using Innova advanced scanning probe microscope (CP-II, Veeco Instruments Inc., USA) in a non-contact tapping mode. A thin film of the sample was prepared on a glass slide by dropping 100 μL of the sample on the slide, and allowed to dry for 5 min. Topographical images were obtained in non-contact mode using silicon nitride tips at a resonance frequency of 218 kHz in ambient air by oscillating the cantilever assembly at or near the cantilever's resonant frequency using a piezoelectric crystal. Characterization was done by observing the patterns on the surface topography and data analysis through WSXM software [24]. The size of the NPs was confirmed by using TEM analysis (Transmission electron microscopy – Hitachi H-7100) using an accelerating voltage of 120 kV and methanol as solvent.

Gas chromatography-mass spectrometry (GC-MS) analysis

The chemical composition of aqueous leaves extract of *E. prostrata* was analyzed using GC-MS (GCD-HP1800A system, Hewlett-Packard, USA) equipped with a split/split less capillary injection port. For GC-MS detection, an electron ionization system (quadrupoles analyzer; mass range, 10–425 amu) with ionization energy of 70 eV was used. Each of these steps carried out under high vacuum from 10⁻⁴ to 10⁻⁸ torr. Helium gas was used as a carrier at a constant flow rate of 1 mL/min. Injector and mass transfer line temperatures were set at 250°C and 280°C, respectively. The components of aqueous leaves extract of *E. prostrata* were identified after comparison with the available data in library (NIST) attached to the GC-MS instrument and reported [25].

Parasite culture and analysis of cell viability

Promastigotes of *L. donovani* strain (MHOM/IN/80/DD8) were routinely cultured as described previously [26]. AlamarBlue[®] cell viability reagent was used for evaluation of antileishmanial activity of synthesized Ag NPs. Logarithmic phase promastigotes of *L. donovani* (50,000 cells, final volume 200 μL/well) were seeded in 96 well microtiter plates (Greiner, bio-one, Germany) in the presence of different concentrations (0, 12.5, 25, 50 and 100 μg/mL) of synthesized Ag NPs and incubated at 25°C for 24 h. Miltefosine was used as the standard drug. 20 μL of AlamarBlue[®] was added to each well and the plate was further incubated at 25°C for 4 h. Absorbance was measured in a ELISA reader (Biotek Instruments, Epoch) using λ=570 nm as test wavelength

(resorufin) and $\lambda=600$ nm as reference wavelength (resazurin) serving as blank. The oxidized form of AlamarBlue[®] resazurin (non-toxic, cell permeable and blue in colour) was reduced by metabolically active cells to resorufin (highly fluorescent, red in colour). Percentage growth inhibition of promastigotes treated with synthesized Ag NPs was analyzed by the following formula [27].

$$\text{Percentage growth inhibition} = \frac{\text{Untreated control } \lambda (570 - 600 \text{ nm}) - \text{treated set } \lambda (570 - 600 \text{ nm})}{\text{untreated control } \lambda (570 - 600 \text{ nm})} \times 100.$$

In vitro antileishmanial activity was expressed as the concentration inhibiting parasite growth by 50% (IC₅₀) and was analyzed by plotting percentage growth inhibition versus log growth concentration (0, 12.5, 25, 50 and 100 $\mu\text{g}/\text{mL}$) of synthesized Ag NPs.

Transmission electron microscopy

TEM analysis was carried out to observe the ultrastructural changes of the morphology of *L. donovani* promastigotes induced by synthesized Ag NPs. Parasites were incubated in the presence of synthesized Ag NPs at IC₅₀ dose for 45 min, washed with PBS (pH 7.2) prior to fixing in 2.5% glutaraldehyde in sodium cacodylate buffer (pH 7.2) for 2 h at 4°C. Fixed parasites were centrifuged at 2000 rpm for 10 min and washed 3 times with 0.1M sodium cacodylate buffer and post fixed in 1% osmium tetroxide for 2 h. Post fixed parasites were washed with sodium cacodylate and dehydrated in ascending acetone series (15, 30, 60 and 100%), embedded in araldite-DDSA mixture and baked at 60°C for 48 h. After baking blocks were cut (60-80 nm thick) by an ultramicrotome (Leica EM UC7, Vienna, Austria), mounted on copper grids and double stained with uranyl acetate and lead citrate. Analysis of stained sections were examined by TEM (TECNAI G2 SPIRIT, FEI, Netherland) equipped with Gatan Orius camera at 80 KV [28].

Propidium iodide uptake assay

Logarithmic phase promastigotes of *L. donovani* (1×10^6 cells, final volume 2 mL/well) were seeded in 6 well microtiter plates (Greiner, bio-one, Germany) in the presence of different concentrations (12.5, 25 and 50 $\mu\text{g}/\text{mL}$) of synthesized Ag NPs and incubated at 25°C for 24 h. After indicated incubation times cells were centrifuged (2000 rpm for 10 min), washed once with PBS (pH 7.2), resuspended in 50 $\mu\text{g}/\text{mL}$ final concentration of PI, and incubated for 30 min in the dark at room temperature. Unbound PI was removed by washing and samples were processed on a FACSCalibur flow cytometer (BD Bioscience, San Jose, CA, USA) and analysed using CellQuest Pro software.

Cell cycle analysis

Briefly 2×10^6 cells/mL log phase *L. donovani* promastigotes were treated with different concentrations (12.5, 25 and 50 $\mu\text{g}/\text{mL}$) of synthesized Ag NPs for 24 h and were harvested by centrifugation at 2000 rpm for 5 min at 4°C. Cells were washed once in 1 mL PBS and then fixed by incubation in 70% ethanol: 30% PBS for 1 h at 4°C. Fixed cells were harvested by centrifugation at 1000 rpm for 10 min at 4°C, washed in 1 mL PBS and resuspended in 1 mL PBS with RNase A (100 $\mu\text{g}/\text{mL}$) and PI (10 $\mu\text{g}/\text{mL}$). The cells were incubated at room temperature for 45 min and then analysed using FACSCalibur flow cytometer (BD Bioscience, San Jose, CA, USA). Cell cycle distribution was modeled using ModFit LT for Mac V3.0 [29].

Analysis of externalized phosphatidylserine

To quantify the percentage of parasites undergoing apoptosis, annexin-V-FITC and necrosis, PI dual staining was performed as per the manufacturer's instructions (AnnexinV-FITC Apoptosis detection

kit, Sigma, MO, USA). In brief 2×10^6 cells/ mL log phase *L. donovani* promastigotes were treated with different concentrations (12.5, 25 and 50 $\mu\text{g}/\text{mL}$) of synthesized Ag NPs for 24 h and cells were centrifuged (2000 rpm for 5 min), washed twice in PBS and resuspended in annexin V binding buffer [10 mM Hepes/NaOH (pH 7.4), 140 mM NaCl and 2.5 mM CaCl₂]. Annexin V-FITC and PI were then added according to the manufacturer's instructions and incubated for 15 min in the dark at 20–25°C. Samples were analyzed on a FACSCalibur flow cytometer and 10,000 events from each sample were acquired to ensure adequate data [29].

DNA fragmentation assay

The fragmentation of DNA into nucleosomal bands, as a function of apoptotic cell death was studied by DNA laddering assay as described previously [29]. Total cellular DNA from promastigotes exposed to different concentrations (12.5, 25 and 50 $\mu\text{g}/\text{mL}$) of synthesized Ag NPs was isolated according to manufacturer's instructions (Apoptotic DNA ladder detection kit, Cat. No. KHO1021, Molecular Probes, USA). The isolated DNA was quantified spectrophotometrically by the absorbance ratio of 260/280 nm and DNA (1 $\mu\text{g}/\text{lane}$) was separated on 1.2% agarose gel containing ethidium bromide in TBE buffer (50 mM; pH 8.0) for 1.5 h at 75 V, visualized under UV light and photographed using a gel documentation system (Genei[™], Uvitech, Cambridge).

Measurement of reactive oxygen species (ROS) level

Intracellular ROS level was measured in *L. donovani* promastigotes as described previously [30]. Briefly, 2×10^6 cells/mL log phase *L. donovani* promastigotes treated with different concentrations of synthesized Ag NPs (12.5, 25 and 50 $\mu\text{g}/\text{mL}$) for 24 h were washed and resuspended in 500 μL of medium M-199 and loaded with the cell permeant probe 2,7-dichlorodihydrofluorescein diacetate (H₂DCFDA) (10 μM) for 30 min at 20–25°C, and fluorescence was monitored. The fluorescent probe H₂DCFDA is one of the most widely used techniques for direct measuring of the redox state of a cell. It is a cell permeable and relatively non-fluorescent molecule. It is also extremely sensitive to the changes in the redox state of a cell and can be used to follow the changes of ROS over time. Activity of cellular esterases cleaves H₂DCFDA into 2,7-dichlorodihydrofluorescein (DCFH₂). Peroxidases, cytochrome c and Fe²⁺ can all oxidize DCFH₂ to 2, 7-dichlorofluorescein (DCF) in the presence of hydrogen peroxide. Accumulation of DCF in the cells was measured by an increase in fluorescence at 530 nm when the sample was excited at 485 nm. Fluorescence at 530 nm was measured using a FACSCalibur flow cytometer (BD Bioscience) and analysed using CellQuest Pro software. It is assumed to be proportional to the concentration of hydrogen peroxide in the cells [29].

Measurement of intracellular non-protein thiols

The probe, 5-chloromethylfluorescein-diacetate (CMFH-DA, Sigma) is a cell permeable, non-fluorescent dye that upon entering the cell, rapidly binds with non-protein thiols and becomes non-permeable; the simultaneous cleavage of the diacetate moiety by cellular esterases yields a fluorescent thioether. Accordingly, the detected fluorescence is directly proportional to the amount of intracellular non-protein thiols [31]. 2×10^6 cells/mL log phase of *L. donovani* promastigotes treated with aqueous leaves extract of *E. prostrata*, synthesized Ag NPs and AgNO₃ solution for 24 h were collected into 1.5 mL micro centrifuge tubes and centrifuged at 700 rpm for 5 min to remove the supernatant. Then the cell pellets were washed with PBS, incubated with 5-chloromethylfluorescein-diacetate in the dark for 15 min at 37°C and analyzed for fluorescence in the FL1 channel, equipped with a

530/30 nm band pass filter by using FACSCalibur flow cytometer (BD Bioscience) and analysed by CellQuest Pro software.

Statistical analysis

The data has been summarized in mean \pm SD. The comparison of group has been done by one way analysis of variance. The groups are compared by Dunnett's test after one way annova. The individual comparison has been done New man/Keuls test. $p=0.05$ has been considered as the level of significance.

Results and Discussion

The green leaves of *E. prostrata* were selected for synthesis of NPs because they are the site of photosynthesis and availability of more H^+ ions to reduce $AgNO_3$ and $TiO(OH)_2$ into Ag NPs and TiO_2 NPs, respectively. The leaves extract of *E. prostrata* was mixed in the aqueous solution of the silver ion complex and it started to change the color from watery to brown due to reduction of silver ion which indicated the formation of Ag NPs. NPs formation was monitored by colour change, despite the fact that colour change has been reported to be the initial evidence of NPs formation [23]. Results of the present study revealed that the overall optimized reaction conditions for the synthesis of Ag NPs were: concentration of aqueous leaves extract = 12 mL, concentration of $AgNO_3$ solution = 88 mL of 1 mM, temperature = 45°C, pH = 9.0, time = 6 h and the maximum absorption peaks observed at 420 nm. Similarly, synthesized TiO_2 NPs were: concentration of aqueous leaves extract = 20 mL, concentration of $TiO(OH)_2$ solution = 80 mL of 5 mM, temperature = 40°C, pH = 8.0, time = 10 h and the maximum absorption peak observed at 305 nm. These results are in good agreement with the previous authors report [23].

Characterization of the synthesized NPs

The synthesized Ag NPs using *E. prostrata* leaves extract was supported by X-ray diffraction measurements. XRD spectrum was compared with the standard confirmed spectrum of Ag particles formed in the present experiments, which were in the form of nanocrystals, as evidenced by the peaks at 2θ values of 38.26°, 44.45°, 64.58° and 77.49° which were indexed to the planes 111, 200, 220 and 311, respectively. The average grain size of Ag NPs formed in the biosynthesis was determined to be 12.82 ± 2.5 nm for the higher intense peak using

Scherrer's formula, $d = 0.89\lambda/\beta \cos\theta$. XRD analysis for the synthesized TiO_2 NPs showed distinct diffraction peaks at 27.63°, 36.27°, 41.43°, 54.49°, 56.80° and 69.16° indexed to the planes 110, 101, 111, 211, 220 and 301, respectively (Figure 1). The average grain size of TiO_2 NPs formed in the biosynthesis was determined to be 83.22 ± 1.50 nm. The sharp peaks and absence of unidentified peaks confirmed the crystallinity and higher purity of prepared NPs. Dubey et al. [32] reported that the size of nano silver as estimated from the full width at half maximum of the (111) peak of silver using the Scherrer formula was 20 – 80 nm. XRD peaks at 2θ value of 25.25° (101) confirm the characteristic facets for anatase form of TiO_2 [33]. This estimation confirmed the hypothesis of particle monocrystallinity. The sharpening of the peaks clearly indicates that the particles were in the nanoregime.

The FTIR spectroscopy is used to probe the chemical composition of the surface and capping agents for the synthesis of NPs. FTIR analysis of synthesized Ag NPs and TiO_2 NPs using the aqueous leaves extract of *E. prostrata* are shown in Figure 2. The synthesized Ag NPs showed the presence of bands due to heterocyclic amine, NH stretch (3431 cm^{-1}), methylene C-H bend (1616 cm^{-1}), gem-dimethyl (1381 cm^{-1}), cyclohexane ring vibrations (1045 cm^{-1}), skeletal C-C vibrations (818 cm^{-1}) and aliphatic iodo compounds, C-I stretch (509 cm^{-1}). The functional groups for *E. prostrata* leaves aqueous extract and synthesized Ag NPs were 548 and 509 cm^{-1} for aliphatic iodo compounds, C-I stretch. Hence, it proves that synthesized Ag NPs have been synthesized with plants compounds involved in the biological reduction of the $AgNO_3$. Similarly, the synthesized TiO_2 NPs showed the presence of bands due to hydroxy group, H-bonded OH stretch (3420 cm^{-1}), methylene C-H asym./sym. stretch (2926 cm^{-1}), secondary amine, NH bend (1618 cm^{-1}), phenol or tertiary alcohol, OH bend (1377 cm^{-1}), cyclic ethers of large rings, C-O stretch (1071 cm^{-1}) and thioethers, CH_3-S- , C-S stretch (649 cm^{-1}). The functional groups of leaves extract and synthesized TiO_2 NPs were 2924 and 2926 cm^{-1} for methylene C-H asym./sym. stretch, 1618 and 1618 cm^{-1} for secondary amine, NH bend. After reduction of $TiO(OH)_2$ the increase in intensity at 2926 cm^{-1} signify the involvement of the around for methylene C-H asym./sym in the reduction process. Hence, it proves that synthesized TiO_2 NPs have been synthesized with *E. prostrata* compounds involved in the biological reduction of the TiO_2 [34].

The synthesized NPs were characterized by AFM for its detail size,

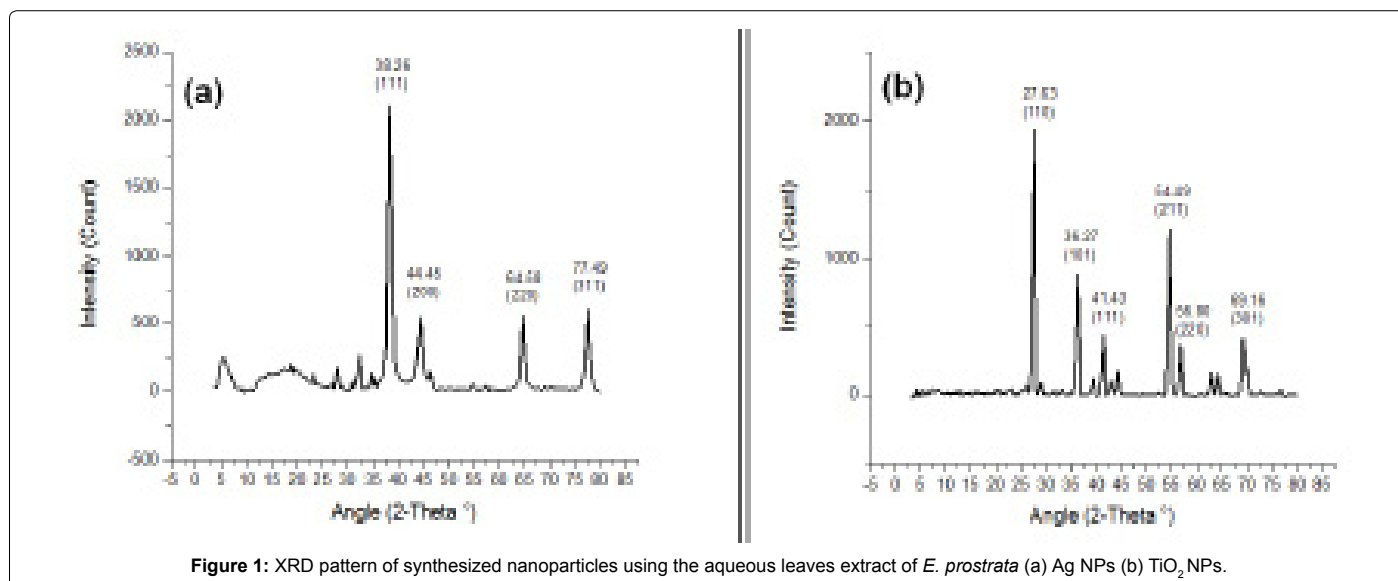


Figure 1: XRD pattern of synthesized nanoparticles using the aqueous leaves extract of *E. prostrata* (a) Ag NPs (b) TiO_2 NPs.

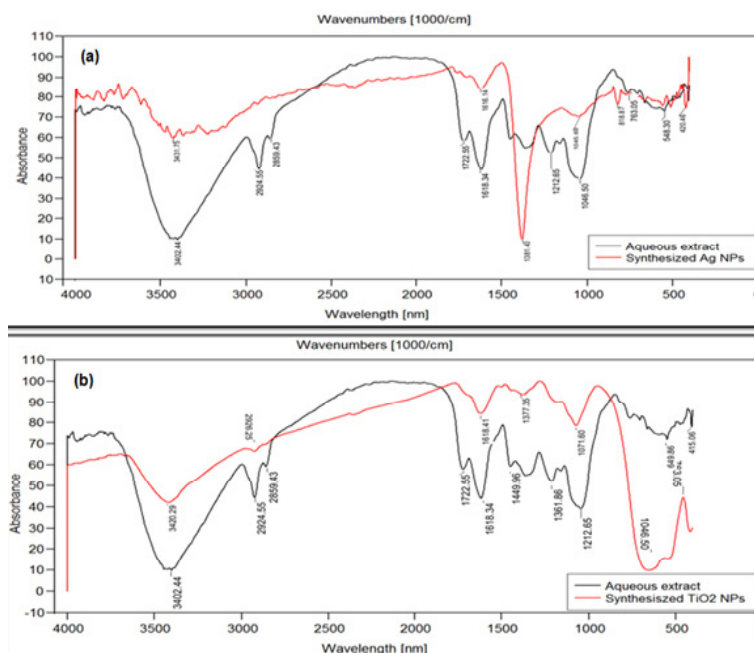


Figure 2: FTIR spectra of vacuum dried powder of synthesized nanoparticles from *E. prostrata* (a) Ag NPs (b) TiO₂ NPs.

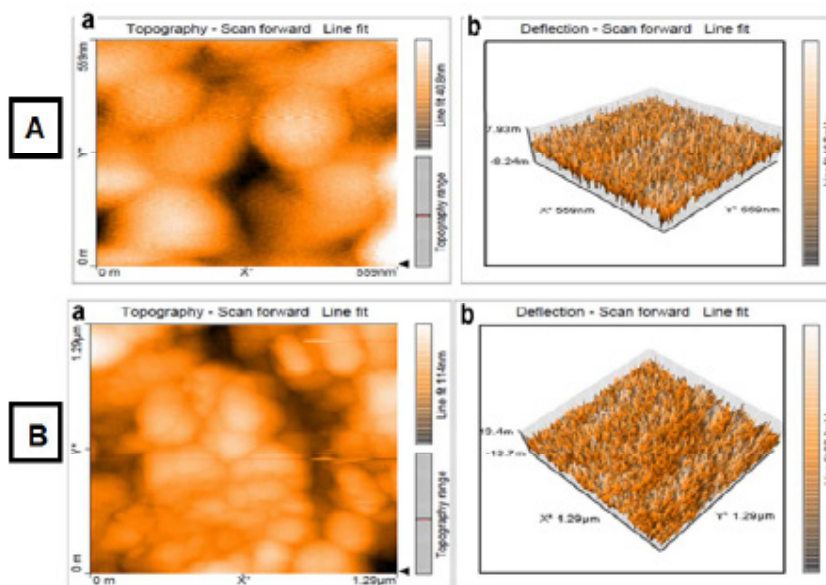


Figure 3: AFM images of the synthesized nanoparticles showing (a) increased surface view and (b) three-dimensional view (A) Ag NPs (B) TiO₂ NPs.

morphology and agglomeration. Characterization of the synthesized NPs using AFM offered a three-dimensional visualization. The uneven surface morphology was explained by the presence of both individual and agglomerated NPs. The strong crystalline nature was observed in the form of diagonal formations with ridges (Figure 3). In accordance with the present results, previous studies have demonstrated that the topographical images of irregular shaped synthesized NPs [35]. TEM images of the synthesized Ag NPs and TiO₂ NPs obtained were spherical, quite polydisperse and individual particles showed an average size of 12.82 ± 2.50 and 83.22 ± 1.50 nm, respectively. SAED pattern of the Ag NPs, the ring-like diffraction pattern indicates that the particles were

crystalline. The diffraction rings were indexed on the basis of the fcc structure of silver. Four rings arise due to reflections from (111), (200), (220) and (311) lattice planes of fcc silver, respectively. SAED pattern of the TiO₂ NPs, six rings arise due to reflections from (110), (101), (111), (211), (220) and (301) lattice planes of fcc titanium, respectively. This is evident by sharp Bragg's reflection observed in the XRD spectrum (Figure 4).

GC-MS analysis

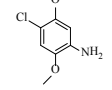
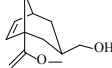
The compounds identified by the GC-MS analysis, the retention time (RT) and percentage peak of the individual compounds in the

aqueous leaves extracts of *E. prostrata* are shown in Table 1. Four compounds were detected in the aqueous leaves extract, the major chemical constituent was identified as 2,3-dihydrobenzofuran (peak area 27.44%) which could have acted as a reducing and capping agent for the synthesis of Ag NPs and TiO₂ NPs. The other constituents such as 1,3-dihydroisobenzofuran (19.97%), 4-chloro-2,5-dimethoxybenzamine (21.80%) and methyl 3-(hydroxymethyl) bicycle [3.2.1] oct-6-ene-1-carboxylate (5.53%) were identified. The chemotherapeutic value of our experimental medicinal plant extract *E. prostrata* is also evident from an earlier study [17]. Previous studies proved that the synthetic dihydrobenzofuran lignans and related benzofurans showed promising antileishmanial compound against *L. donovani* [36].

Analysis of cell viability

Considering the efficacy of drugs available for the treatment of VL as well as their side effects and the resistance developed by parasites, the research in phytosciences, mainly regarding the properties of bioactive phytochemicals found in the crude extracts of medicinal plants, may lead to the discovery of new medicines with appropriate efficiency which are cheap and safe to the patients. Hence the purpose of this research was to study the antileishmanial effects of synthesized Ag NPs and TiO₂ NPs against *L. donovani* parasites. The results showed that the synthesized Ag NPs were most active against promastigotes of *L. donovani* compared to aqueous leaves extract of *E. prostrata*, AgNO₃ and TiO(OH)₂ solutions and synthesized TiO₂ NPs. Significance level were estimated by one way ANOVA followed by Dunnett's multiple comparison test and found to be highly significant (p<0.001) for synthesized Ag NPs (Table 2). Decreased mobility of promastigotes treated with aqueous leaves extract of *E. prostrata*, synthesized Ag NPs and AgNO₃ solution were observed under light microscope in the first 24 h of treatment. Pronounced morphological changes within the parasite such as round to oval, shape decrease in size with dense cytoplasm and enlarged nuclei were also observed. Soon after 24 h, the morphology of the treated promastigotes was completely destroyed.

The IC₅₀ values were determined at 24 h of treatment with synthesized Ag NPs. The result showed the IC₅₀ log value of 1.17 µg/mL which is equivalent to 14.94 µg/mL (Figure 5). Previous studies proved that the Ag NPs demonstrated significant antileishmanial effects by inhibiting

RT	Identified molecules	Chemical structure	MF	MW	Peak area %
3.3	2,3- dihydrobenzofuran		C ₈ H ₈ O	120	27.44
4.3	1,3- dihydro isobenzofuran		C ₈ H ₈ O	120	19.97
18.5	4- cholro-2,5- dimethoxybenzamine		C ₉ H ₁₀ ClNO ₂	187	21.80
22.6	Methyl 3-(hydromethyl) bicycle [3.2.1]oct-6-ene-1-carboxylate		C ₁₀ H ₁₄ O ₃	182	5.53

RT: Retention time; MF: Molecular formula; MW: Molecular weight.

Table 1: Chemical composition of the *E. prostrata* leaves extract identified by GC-MS.

Factor	Mean	Standard deviation	p-value
Ag NPs	0.255	0.015	p<0.001
TiO ₂ NPs	0.653	0.001	p<0.001
Aqueous extract	0.359	0.007	p<0.001
AgNO ₃	0.320	0.003	p<0.01
TiO(OH) ₂	0.747	0.018	p<0.001
Control	0.989	0.016	p<0.001

The significance between synthesized Ag NPs and aqueous leaves extract of *E. prostrata*, AgNO₃, and TiO(OH)₂ solutions and synthesized TiO₂ NPs (Factor). Lowest percentage cell viability was found with synthesized Ag NPs. It was significantly lower than all other factor.

Table 2: The mean % cell viability test by one way ANOVA and Dunnett's multiple comparison test.

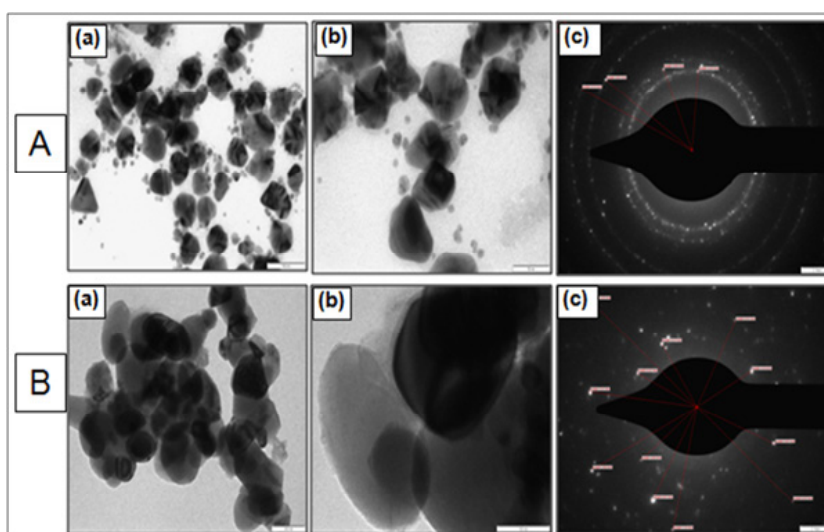


Figure 4: (A) TEM micrograph of the synthesized Ag NPs formed with 12.82 ± 2.5 nm using 12 mL aqueous leaves extract of *E. prostrata* mixed with 88 mL of 1 mM aqueous AgNO₃ solution at 45°C and pH 9 at two different magnification (a) 100 nm (b) 50 nm and (c) Selected area electron diffraction of the Ag NPs showed four rings arise due to reflections from (111), (200), (220) and (311) lattice planes of fcc silver, respectively (B) TEM micrograph of the synthesized TiO₂ NPs formed with 83.22 ± 1.5 nm using 20 mL aqueous leaves extract of *E. prostrata* mixed with 80 mL of 5 mM TiO(OH)₂ solution at 45°C and pH 8 at different magnification (a) 200 nm (b) 100 nm and (c) Selected area electron diffraction pattern of TiO₂ NPs showed six rings arise due to reflections from (110), (101), (111), (211), (220) and (301) lattice planes of fcc titanium, respectively.

the proliferation and metabolic activity of promastigotes form of *L. tropica* under UV light [11].

Transmission electron microscopy

The TEM study has been the most widely used techniques to visualize agglomerated NPs in cells. The ultrastructural analysis of the promastigotes treated with synthesized Ag NPs showed cytolysis with features of necrosis including a general cell hydration causing swelling of the organelles (endoplasmic reticulum and mitochondria),

vacuolization, and gross alterations in the organization of the nuclear and chromatin when compared to control (Figure 6). Asharani et al. [37] reported that the Ag NPs are also known to accumulate heavily within mitochondria and are reported to impair mitochondrial function via oxidative stress.

Propidium iodide uptake assay

Cytotoxicity of different concentrations of synthesized Ag NPs was evaluated by measuring cellular uptake of PI in *L. donovani* promastigotes

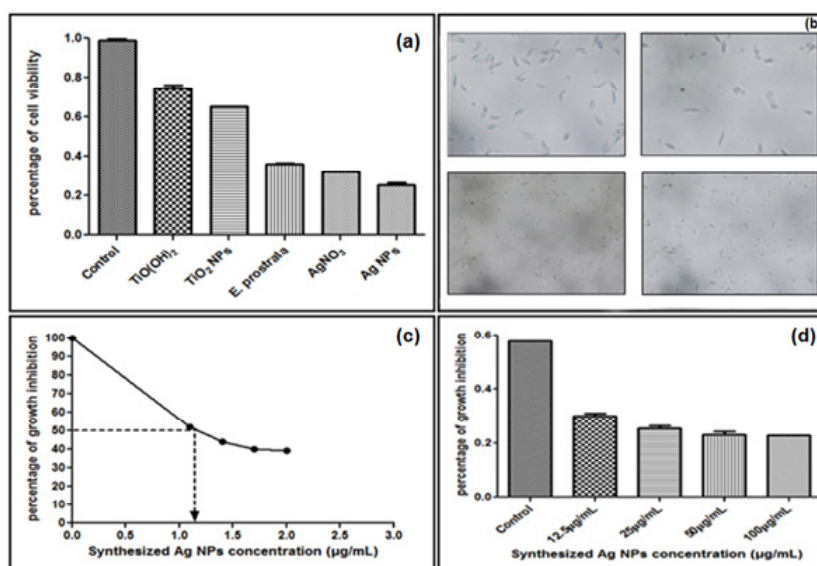


Figure 5: Cell viability assessment by alamarBlue® shows reduction in viability with different concentrations (0, 25, 50 and 100 µg/mL) of synthesized Ag NPs treated promastigotes (a) Graph shows that the synthesized Ag NPs were most active against promastigotes of *L. donovani* compared to aqueous leaves extract, AgNO₃ and TiO(OH)₂ solutions and synthesized TiO₂ NPs (b) Microscopic images of wild type promastigotes and promastigotes treated with aqueous leaves extract of *E. prostrata*, AgNO₃ solution and synthesized Ag NPs at a magnification of 60X (c) Percentage growth inhibition against log value of synthesized Ag NPs concentrations (µg/mL), IC₅₀ = 14.94 µg/mL (d) Percentage growth inhibition of *L. donovani* promastigotes treated with synthesized Ag NPs concentrations. The data are presented as means ± standard deviation of three independent experiments.

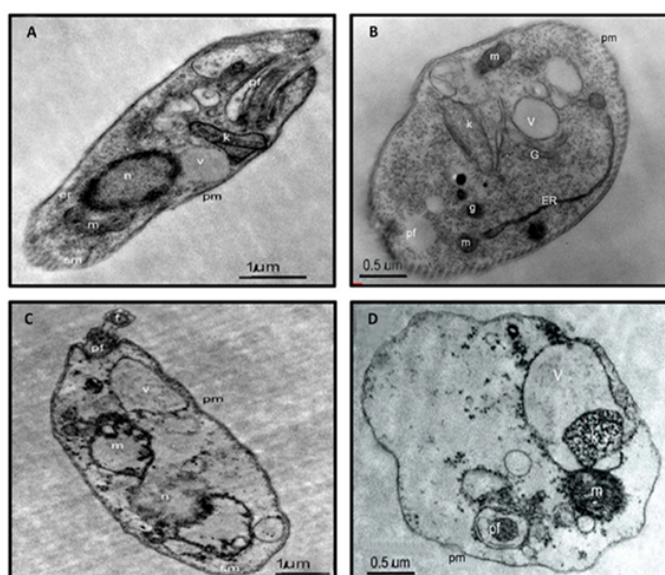


Figure 6: Transmission electron microscopy of *L. donovani* promastigotes (a and b) incubated with vehicle and (c and d) synthesized Ag NPs at IC₅₀ dose for 45 min, n: nucleus; k: kinetoplast; m: mitochondria; pf: pocket flagellar; pm: plasma membrane; G: golgi body; g: glycosome; ER: endoplasmic reticulum. Scale bars 1.0 µm and 0.5 µm.

after 24 h treatment. PI uptake was used to quantify the population of cells in which membrane integrity was lost resulting in cell death. Treated promastigotes undertaken PI in a concentration-dependent manner. Figure 7 shows sharp increase in PI positive (M2) cells from 19.27% at 12.5 µg/mL to 50.36% at 25 µg/mL and thereafter gradual decrease to 48.01% at 50 µg/mL after 24 h of treatment. Untreated cells which served as control showed no cell death. These results are consistent with those of other studies and suggested that the cytotoxic effect induced by biosynthesized Ag NPs involved apoptotic changes and the nuclear condensation was studied by the propidium iodide staining method [38].

Cell cycle analysis

To assess the role of different concentrations (12.5, 25 and 50 µg/mL) of synthesized Ag NPs in mediating G0/G1 arrest and the present study performed cell cycle analysis by flow cytometry after PI staining

of the parasites incubated for 24 h, as described previously by us [39]. Figure 8 shows that synthesized Ag NPs (at 12.5 and 25 µg/mL) induced a marked increase in the number of cells in the G0/G1 phase (G1:48.69% versus 60.50% to 62.00%), and simultaneous decrease in both S phase (S: 33.86% versus 31.73% to 27.70%) and G2/M phase compared with control was observed (G2/M: 17.44% versus 7.76% to 10.30%). The concentration-dependent effect on G0/G1 arrest in promastigotes was largely at the expense of S phase cells, with low change in the G2/M-phase cell population compared with the untreated promastigotes. The drug-induced cell cycle perturbations, such as an increase in the number of cells in the G1 phase, have been reported to correlate with a response to chemotherapy [40].

Analysis of externalized phosphatidylserine

To delineate the nature of cell death, *L. donovani* promastigotes

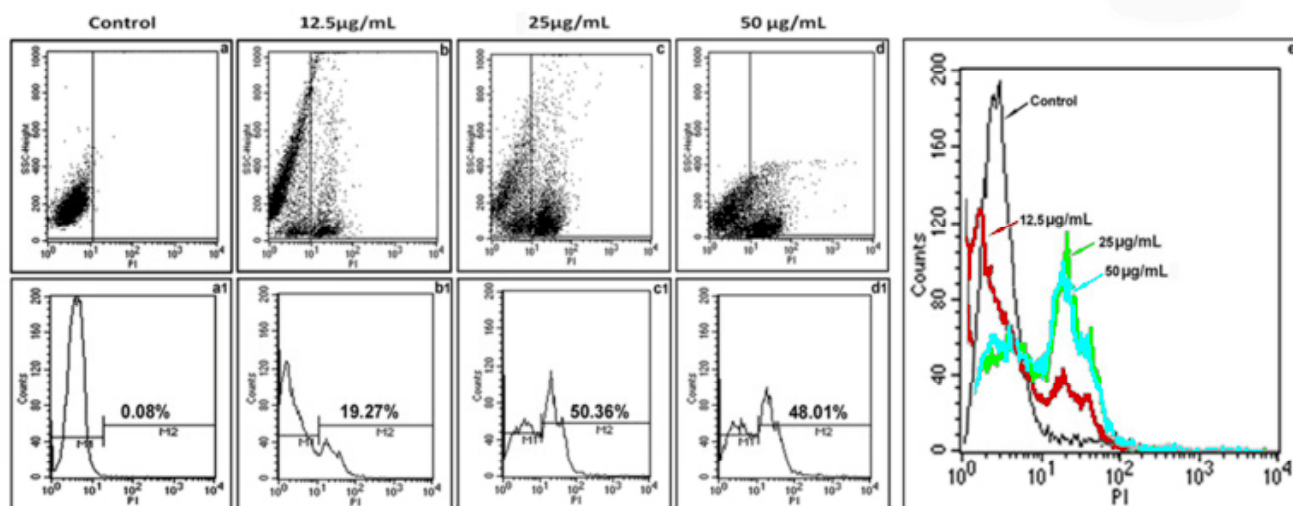


Figure 7: PI uptake analysis of *L. donovani* promastigotes treated with different concentrations of synthesized Ag NPs. Dot plots (a, b, c and d) show that treatment of *Leishmania* parasites with synthesized Ag NPs leads to (PI-positive cells M2) (a1,b1,c1 and d1) cell death in a concentration-dependent manner.

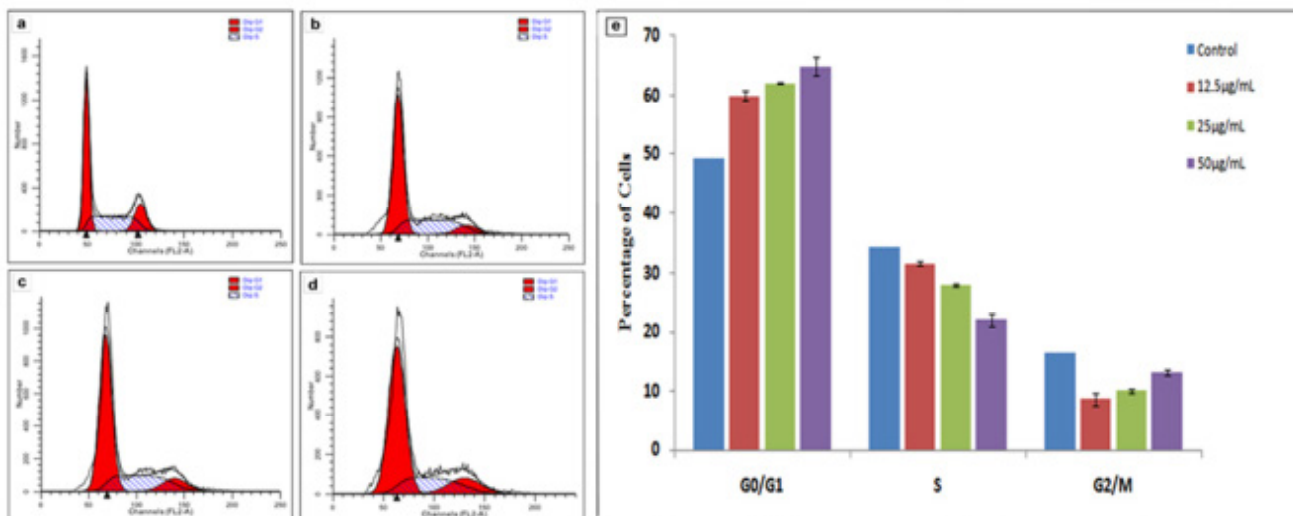
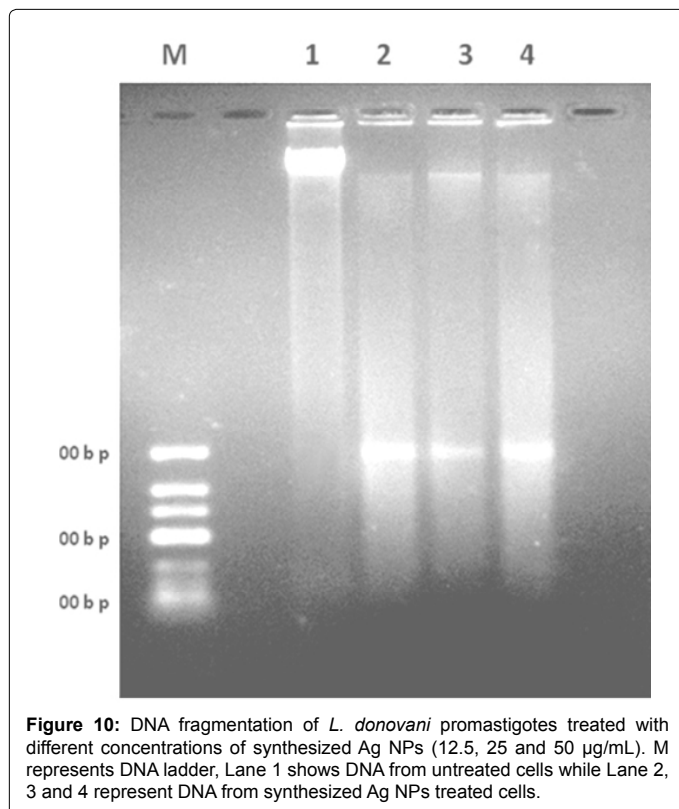
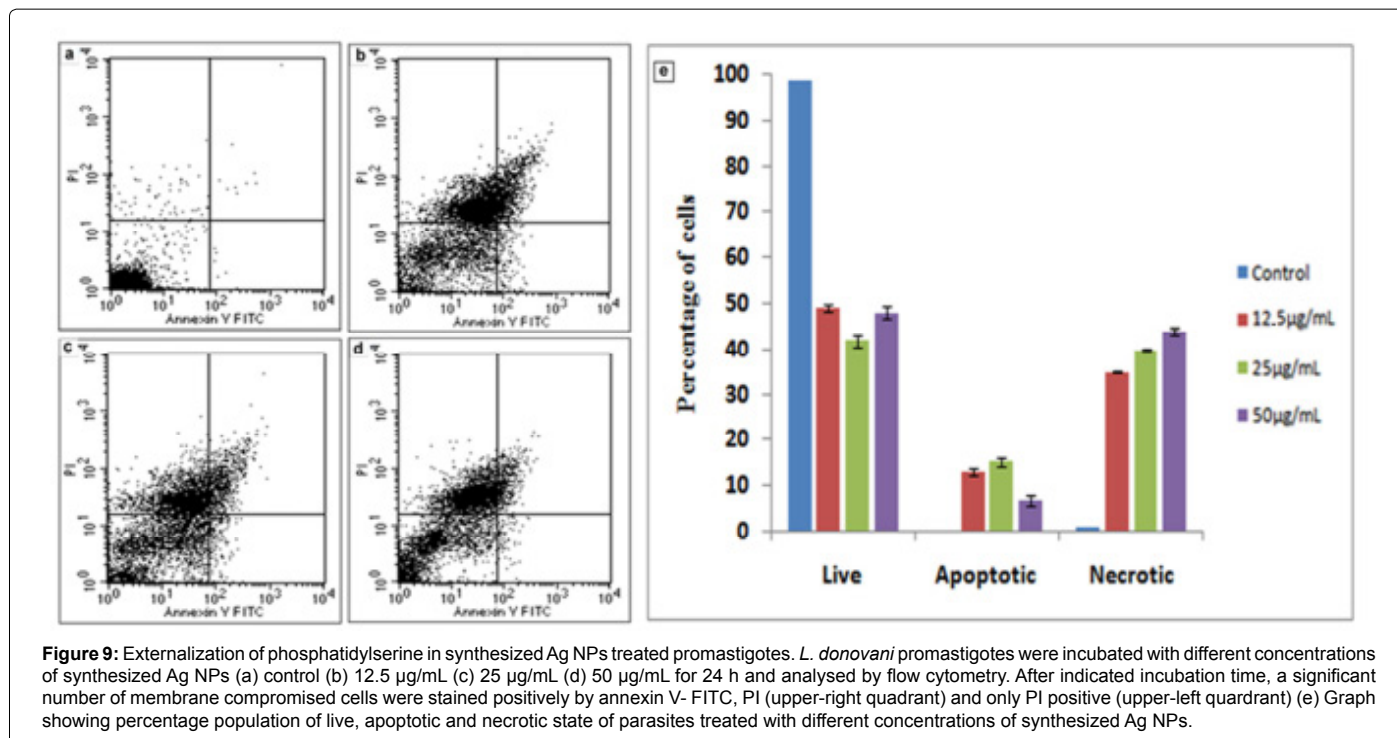


Figure 8: Synthesized Ag NPs induced cell cycle arrest in the G0/G1 phase of *L. donovani* parasites. After treatment with different concentrations of synthesized Ag NPs (a, b, c and d) for 24 h, promastigotes were collected, washed with PBS and stained with PI, the DNA content was analysed by flow cytometry (e) Graph showing % population in G0/G1, S and G2/M phase of parasites treated with different concentrations (12.5, 25 and 50 µg/mL) of synthesized Ag NPs.



which were treated with different concentrations (12.5, 25 and 50 µg/mL) of synthesized Ag NPs for 24 h were harvested, washed with PBS and double-stained with annexin V-FITC and PI. The number of cells that were PI-positive (upper-left quadrant) gradually increased from 34.87, 39.90 and 44.01% at 12.5, 25 and 50 µg/mL, respectively. These

observations suggested that synthesized Ag NPs induced cell death by necrosis. The synthesized Ag NPs treated promastigotes showed positive for both annexin V and PI-positive (upper-right quadrant) and decreased the activity of 13.12, 15.17 and 6.78% at 12.5, 25 and 50 µg/mL, respectively (Figure 9). In contrast, only 0.18% of untreated cells, which served as control were annexin V and PI-positive and showed no cell death. These results are a confirmatory indication of shift from apoptosis to necrosis on treatment of *L. donovani* promastigotes with synthesized Ag NPs. Fluorescein-conjugated annexin-V was used to detect externalized phosphatidylserine as it has a high binding affinity to this phospholipid component. Annexin-V showed the percentage of apoptotic, necrotic and surviving cells. Khademvatan et al. [41] reported that the Annexin V- FLUOS staining induced apoptotic phenomenon in promastigotes of *Leishmania major* using FACS flow cytometry.

DNA fragmentation assay

Treatment of promastigotes with different concentrations (12.5, 25 and 50 µg/mL) of synthesized Ag NPs for 24 h and revealed DNA breakage which was not extensive. High molecular weight DNA fragments ~700 bp were observed (Figure 10), which reconfirmed that mode of cell death in promastigotes may be largely due to necrosis. In the present study, synthesized Ag NPs using the aqueous leaves extracts of *E. prostrata* for 24 h, revealed DNA breakage which was not extensive. Previous reports showed that the Ag NPs were found to increase the DNA tail length in a comet assay, which measures DNA strand breaks as well as alkali labile sites [42].

Formation of ROS in *L. donovani*

An inherent basic level of ROS production in wild type promastigotes was detected with mean fluorescence intensity of 82.66%. Treatment of promastigotes with synthesized Ag NPs for 24 h revealed a gradual decrease in ROS generation from 34.35, 30.42 and 27.96% at 12.5, 25 and 50 µg/mL, respectively with respect to control cells (Figure 11). However, the present study showed the decreased ROS production

in the synthesized Ag NPs treated parasites which was responsible for caspase independent necrotic cell death mechanism. An established event in most apoptotic cells was the generation of ROS in the cytosol, which directs the cell and its neighboring cells towards the path of apoptotic cell death [43]. Lower levels of ROS in our study could be a result of the antioxidant activity of the aqueous leaves extract of *E. prostrata* which constituted the synthesized Ag NPs. Presumably this effect resulted in a shift from apoptosis to G0/G1 arrest followed by necrotic cell death in *L. donovani*.

Measurement of intracellular non-protein thiols

The fluorescent probe, 5-chloromethyl fluorescein diacetate was

used to measure total intracellular non-protein thiols after treatment of *L. donovani* promastigotes with aqueous leaves extract of *E. prostrata*, synthesized Ag NPs and AgNO₃ solution. Synthesized Ag NPs showed remarkable decrease (3.55%) in comparison with the control cells (219.69%) at 24 h. On analysis of our results we found that intracellular non protein thiols increase (261.16%) in comparison with the wild type cells (219.69%) was presumably a result of the antioxidant activity of the aqueous leaves extract of *E. prostrata*. Also, Ag was known to be an excellent effective Trypanothione reductase (TR) inhibitor. In the present observations, AgNO₃ treated cells were obtained a remarkable decrease (5.67%) in comparison with the wild type cells (219.69%) (Figure 12). The glutathione/glutathione reductase

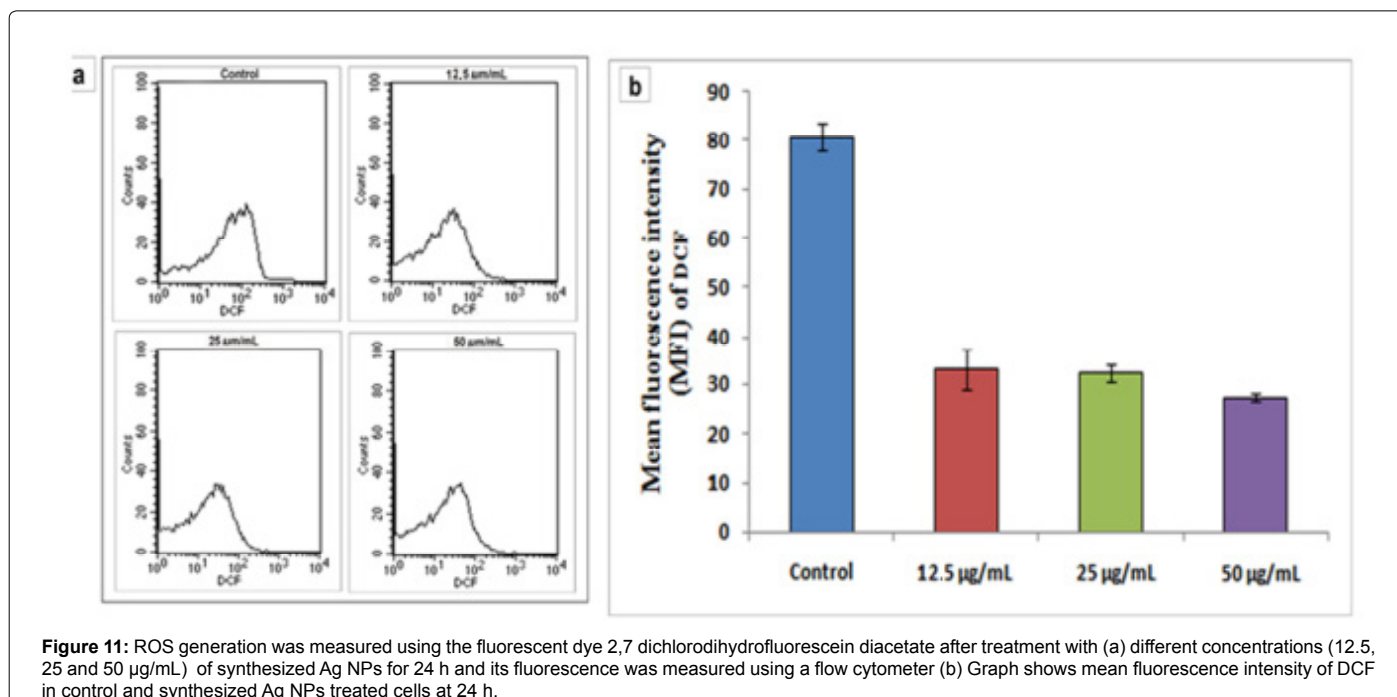


Figure 11: ROS generation was measured using the fluorescent dye 2,7 dichlorodihydrofluorescein diacetate after treatment with (a) different concentrations (12.5, 25 and 50 µg/mL) of synthesized Ag NPs for 24 h and its fluorescence was measured using a flow cytometer (b) Graph shows mean fluorescence intensity of DCF in control and synthesized Ag NPs treated cells at 24 h.

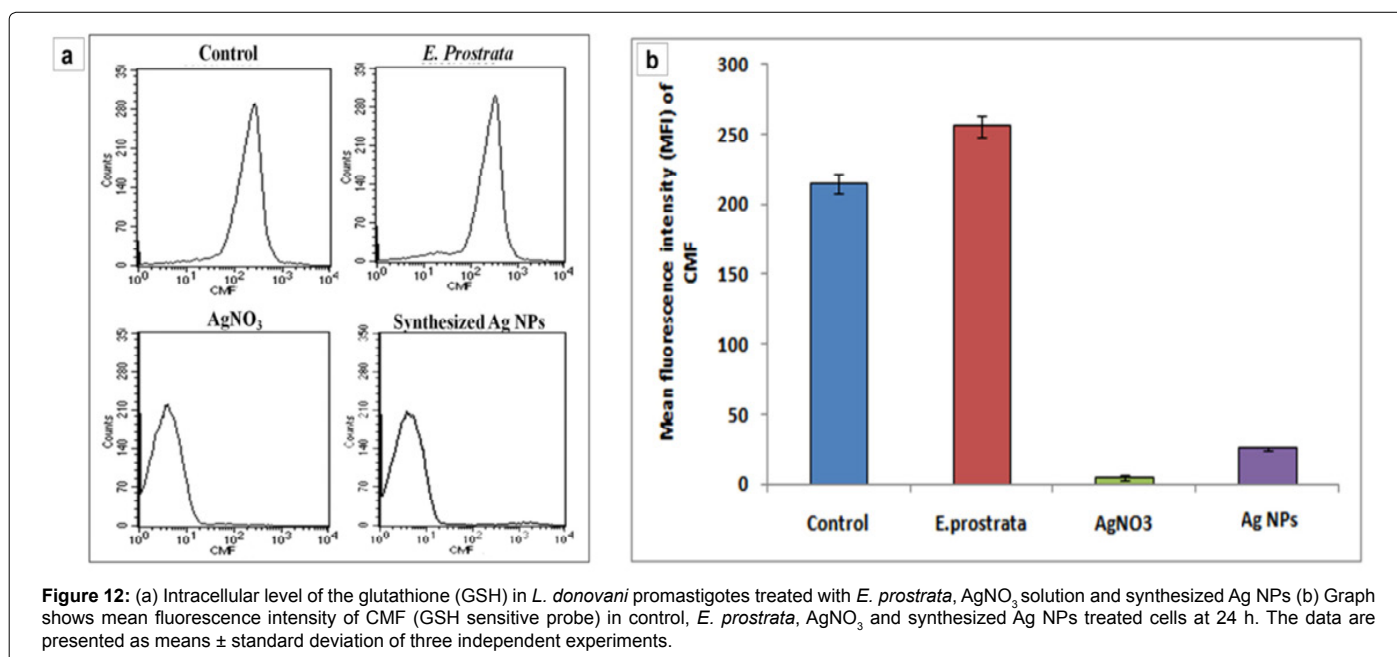


Figure 12: (a) Intracellular level of the glutathione (GSH) in *L. donovani* promastigotes treated with *E. prostrata*, AgNO₃ solution and synthesized Ag NPs (b) Graph shows mean fluorescence intensity of CMF (GSH sensitive probe) in control, *E. prostrata*, AgNO₃ and synthesized Ag NPs treated cells at 24 h. The data are presented as means ± standard deviation of three independent experiments.

eukaryotic redox system was replaced by the unique TR system against *L. donovani*. Earlier authors reported that the Ag NPs was known to be an excellent effective TR inhibitor [44]. This was also corroborated by our results which showed maximum TR inhibition in synthesized Ag NPs treated promastigotes in comparison to aqueous leaves extract of *E. prostrata* treated promastigotes. It has been established that 2,3-dihydrobenzofuran, the main chemical constituent of plant extract of *E. prostrata* was also a promising antileishmanial lead molecule and contains antitubulin properties [45]. This drug target of the parasite has a different primary amino acid sequence to that of its host. The depletion of intracellular non-protein thiols in *Leishmania* parasites treated with synthesized Ag NPs was independent of ROS generation. Our study therefore shows the important benefit of taking up these synthesized Ag NPs further for clinical development as our green synthesized NPs has advantage of prevention of development of drug resistance.

Conclusions

The present finding revealed that the aqueous leaves extracts of *E. prostrata* are capable of synthesizing NPs from inorganic salts would also provide a clue as to one of the probable ways by which the drug may act inside the living systems. Thus, it seems quite possible that if we extrapolate the results of the present investigation, the leaves extracts of *E. prostrata* may also be capable of synthesizing NPs from some inorganic salts available in the living system and which in turn could have some role in eliciting the medicinal responses to remove the disease/disease symptoms. The results are very promising since the extract promotes the formation of NPs at room temperature with a fast kinetics and with no harmful chemicals. In conclusion, this study affirm from our studies that the synthesized Ag NPs were potent active against promastigotes of *L. donovani* compared with TiO₂ NPs, aqueous leaves extracts and bulk solutions. The potent leishmanicidal effect of the active synthesized Ag NPs from the aqueous leaves extract may provide promising leads for the development of new and safer drugs against visceral leishmaniasis in near future.

Acknowledgments

The authors are grateful to C. Abdul Hakeem College Management, Dr. K. Masood Ahmed Principal, and Dr. Hameed Abdul Razack, Head of Zoology Department for providing the facilities to carry out this work. The technical assistance of Mr. A.L. Vishwakarma regarding flow cytometry is acknowledged. This work was supported by Council of Scientific and Industrial Research (CSIR) funded network project "Host Interactome analysis: Understanding the Role of Host molecules in Parasitic Infection (HOPE)."

This is CDRI communication no. 80/2014/NS.

References

1. http://www.who.int/leishmaniasis.disease_epidemiology/en/index.html
2. Richard JV, Werbovetz KA (2010) New antileishmanial candidates and lead compounds. *Curr Opin Chem Biol* 14: 447-455.
3. Ezra N, Ochoa MT, Craft N (2010) Human immunodeficiency virus and leishmaniasis. *J Glob Infect Dis* 2: 248-257.
4. Kim BY, Rutka JT, Chan WC (2010) Nanomedicine. *N Engl J Med* 363: 2434-2443.
5. Irache JM, Esparza I, Gamazo C, Agüeros M, Espuelas S (2011) Nanomedicine: novel approaches in human and veterinary therapeutics. *Vet Parasitol* 180: 47-71.
6. Morones JR, Elechiguerra JL, Camacho A, Holt K, Kouri JB, et al. (2005) The bactericidal effect of silver nanoparticles. *Nanotechnology* 16: 2346-2353.
7. Sinha S, Pan I, Chanda P, Sen SK (2009) Nanoparticles fabrication using ambient biological resources. *J Appl Biosci* 19: 1113-1130.
8. Bhainsa KC1, D'Souza SF (2006) Extracellular biosynthesis of silver nanoparticles using the fungus *Aspergillus fumigatus*. *Colloids Surf B Biointerfaces* 47: 160-164.
9. Mohebbali M, Rezayat MM, Gilani K, Sarkar S, Akhouni B, et al. (2009) Nanosilver in the treatment of localized cutaneous leishmaniasis caused by *Leishmania major* (MRHO/IR/75/ER): an *in vitro* and *in vivo* study. *J Pharmaceutical Sci* 17: 285-289.
10. Zampa MF, Araújo IM, Costa V, Nery Costa CH, Santos JR Jr, et al. (2009) Leishmanicidal activity and immobilization of dermaseptin 01 antimicrobial peptides in ultrathin films for nanomedicine applications. *Nanomedicine* 5: 352-358.
11. Allahverdiyev AM, Abamor ES, Bagirova M, Ustundag CB, Kaya C, et al. (2011) Antileishmanial effect of silver nanoparticles and their enhanced antiparasitic activity under ultraviolet light. *Int J Nanomed* 6: 2705-2714.
12. Torabi N, Mohebbali M, Shahverdi AR, Rezayat SM, Edrissian GH, et al. (2011) Nanogold for the treatment of zoonotic cutaneous leishmaniasis caused by *Leishmania major* (MRHO/IR/75/ER): an animal trial with methanol extract of *Eucalyptus camaldulensis*. *J Pharmaceutical Health Sci* 1: 13-16.
13. Navarro L, Dunoyer P, Jay F, Arnold B, Dharmasiri N, et al. (2006) A plant miRNA contributes to antibacterial resistance by repressing auxin signaling. *Science* 312: 436-439.
14. Wiesenthal A, Hunter L, Wang S, Wickliffe J, Wilkerson M (2011) Nanoparticles: small and mighty. *Int J Dermatol* 50: 247-254.
15. Das S, Roy P, Mondal S, Bera T, Mukherjee A (2013) One pot synthesis of gold nanoparticles and application in chemotherapy of wild and resistant type visceral leishmaniasis. *Colloids Surf B Biointerfaces* 107: 27-34.
16. Sundrarajan M, Gowri S (2011) Green synthesis of titanium dioxide nanoparticles by *Nyctanthes arbor-tristis* leaves extract. *Chalcogenide Lett* 8: 447-451.
17. Schmelzer GH, Gurib-Fakim A (2008) Plant resources of tropical Africa medicinal plants 1, Backhuys publishers, Netherlands, 287.
18. Kamgang R, Hortense GK, Pascal W (2007) Activity of aqueous ethanol extract of *Euphorbia prostrata* ait on *Shigella dysenteriae* type 1- induced diarrhea in rats. *Indian J Pharmacol* 39: 240-244.
19. Kerboeuf D, Riou M, Guégnard F (2008) Flavonoids and related compounds in parasitic disease control. *Mini Rev Med Chem* 8: 116-128.
20. Radtke OA, Foo LY, Lu Y, Kiderlen AF, Kolodziej H (2003) Evaluation of sage phenolics for their antileishmanial activity and modulatory effects on interleukin-6, interferon and tumour necrosis factor-alpha-release in RAW 264.7 cells. *Z Naturforsch C* 58: 395-400.
21. Sharma U, Singh D, Kumar P, Dobhal MP, Singh S (2011) Antiparasitic activity of plumericin & isoplumericin isolated from *Plumeria bicolor* against *Leishmania donovani*. *Indian J Med Res* 134: 709-716.
22. Parashar UK, Saxena PS, Srivastava A (2009) Bioinspired synthesis of silver nanoparticles. *Dig J Nanomater Biostruct* 4: 159-166.
23. Veerasamy R, Xin TZ, Gunasagaran S, Xiang TFW, Yang EFC, et al. (2011) Biosynthesis of silver nanoparticles using mangosteen leaf extract and evaluation of their antimicrobial activities. *Saudi Chem Soc* 15: 113-120.
24. Horcas I, Fernández R, Gómez-Rodríguez JM, Colchero J, Gómez-Herrero J, et al. (2007) WSXM: a software for scanning probe microscopy and a tool for nanotechnology. *Rev Sci Instrum* 78: 013705.
25. Suresh C, Senthilkumar S, Vijayakumari K (2012) GC-MS analysis of *Tephrosia purpurea* pers leaf extract- traditional valuable plant. *Int J Uni Pharm Life Sci* 2: 86-91.
26. Kaur J, Sundar S, Singh N (2010) Molecular docking, structure – activity relationship and biologic evaluation of the anticancer drug monastrol as a peridine reductase inhibitor in a clinical isolate of *Leishmania donovani*. *J Antimicrob Chemother* 65: 1742-1748.
27. Ghosh S, Debnath S, Hazra S, Hartung A, Thomale K, et al. (2011) *Valeriana wallichii* root extracts and fractions with activity against *Leishmania* spp. *Parasitol Res* 108: 861-871.
28. do Socorro S Rosa Mdo S, Mendonça-Filho RR, Bizzo HR, de Almeida Rodrigues I, Soares RM, et al. (2003) Antileishmanial activity of a linalool-rich essential oil from *Croton cajucara*. *Antimicrob Agents Chemother* 47: 1895-1901.
29. Kaur J, Singh BK, Tripathi RP, Singh P, Singh N (2009) *Leishmania donovani*: a glycosyl dihydropyridine analogue induces apoptosis like cell death via targeting peridine reductase 1 in promastigotes. *Exp Parasitol* 123: 258-264.

30. Mukherjee SB, Das M, Sudhandiran G, Shaha C (2002) Increase in cytosolic Ca^{2+} levels through the activation of non-selective cation channels induced by oxidative stress causes mitochondrial depolarization leading to apoptosis-like death in *Leishmania donovani* promastigotes. J Biol Chem 277: 24717-24727.
31. Sarkar A, Mandal G, Singh N, Sundar S, Chatterjee M (2009) Flow cytometric determination of intracellular non-protein thiols in *Leishmania* promastigotes using 5-chloromethyl fluorescein diacetate. Exp Parasitol 122: 299-305.
32. Dubey M, Bhadauria S, Kushwah BS (2009) Green synthesis of nanosilver particles from extract of *Eucalyptus hybrida* (safeda) leaf. Dig J Nanomater Biostruct 4: 537-543.
33. Liu Z, Hong L, Guo B (2005) Physicochemical and electrochemical characterization of anatase titanium dioxide NPs. J Power Sources 143: 231-235.
34. Coates J (2000) In: Meyers RA (edn) Interpretation of infrared spectra, a practical approach. Encyclopedia of analytical chemistry. Wiley, Chichester, 10815-10837.
35. Logeswari P, Silambarasan S, Abraham J (2012) Synthesis of silver nanoparticles using plants extract and analysis of their antimicrobial property. J Saudi Chem Soc.
36. Van Miert S, Van Dyck S, Schmidt TJ, Brun R, Vlietinck A, et al. (2005) Antileishmanial activity, cytotoxicity and QSAR analysis of synthetic dihydrobenzofuran lignans and related benzofurans. Bioorg Med Chem 13: 661-669.
37. AshaRani PV, Low Kah Mun G, Hande MP, Valiyaveetil S (2009) Cytotoxicity and genotoxicity of silver nanoparticles in human cells. ACS Nano 3: 279-290.
38. Prabhu D, Arulvasu C, Babu G, Manikandan R, Srinivasan P (2013) Biologically synthesized green silver nanoparticles from leaf extract of *Vitex negundo* L. induce growth-inhibitory effect on human colon cancer cell line HCT15. Process Biochem. 48: 317-324.
39. Kaur J, Dutta S, Chang KP, Singh N (2013) A member of the Ras oncogene family, RAP1A, mediates antileishmanial activity of monastrol. J Antimicrob Chemother 68: 1071-1080.
40. Efuot ET, Keyomarsi K (2006) Farnesyl and geranylgeranyl transferase inhibitors induce G1 arrest by targeting the proteasome. Cancer Res 66: 1040-1051.
41. Khademvatan S, Saki J, Gharavi MJ, Rahim F (2011) *Allium sativum* extract induces apoptosis in *Leishmania major*. J Med Plants Res 5: 3725-3732.
42. Premanathan M, Karthikeyan K, Jeyasubramanian K, Manivannan G (2011) Selective toxicity of ZnO nanoparticles toward Gram-positive bacteria and cancer cells by apoptosis through lipid peroxidation. Nanomed: Nanotechnol Biol Med 7: 184-192.
43. Chipuk JE, Green DR (2005) Do inducers of apoptosis trigger caspase-independent cell death? Nat Rev Mol Cell Biol 6: 268-275.
44. Baiocco P, Ilari A1, Ceci P1, Orsini S2, Gramiccia M2, et al. (2010) Inhibitory Effect of Silver Nanoparticles on Trypanothione Reductase Activity and *Leishmania infantum* Proliferation. ACS Med Chem Lett 2: 230-233.
45. Van Miert S, Van Dyck S, Schmidt TJ, Brun R, Vlietinck A, et al. (2005) Antileishmanial activity, cytotoxicity and QSAR analysis of synthetic dihydrobenzofuran lignans and related benzofurans. Bioorg Med Chem 13: 661-669.